PERGAMON

International Journal of Heat and Mass Transfer 42 (1999) 2363–2374

International Journal of HEAT and MASS TRANSFER

3-D numerical modeling of heat transfer between two sliding bodies: temperature and thermal contact resistance

B. Salti*, N. Laraqi

Université Paris VI, URA CNRS 879, LMP, Equipe 'Transferts Thermiques', T.66, BP. 160, 4-Place Jussieu, 75252 Paris Cedex 05, France

Received 23 January 1997; in final form 11 September 1998

Abstract

A three-dimensional numerical model using the finite volume method was developed to calculate the steady-state temperatures and the thermal contact resistance between two sliding bodies: one is rough and stationary, the other is smooth and moving at a velocity V. The roughness is represented by square-shaped asperities characterized by a parameter ε. Heat transfers through interstitial gaps are not taken into account. The numerical methodology was particularly studied in order to reduce the computation time and obtain accurate results. This model was validated by comparison of results with those of an analytical solution.

Key words: Thermal contact resistance; Numerical modeling in moving bodies; Sliding contact

Nomenclature

A_a apparent contact area of an elementary cell
A_r real contact area of an elementary cell
e width
e' width of the modeled domain
h heat convection coefficient
h' heat conductance
k thermal conductivity
l half-width of the real contact area
L half-width of the apparent contact area
N number of meshes
q heat flux per unit area
Q heat flux ($= q(2l)^2$)
R thermal resistance
T temperature
T_e ambient temperature
T^* dimensionless temperature ($=(T-T_e)(qL/k)$)
V sliding velocity
V^* dimensionless velocity ($=V(2L/\alpha)$)
x, y, z space coordinates.

Greek symbols
α thermal diffusivity
δ asperity height
Δ space step
ε relative contact size ($=\sqrt{A_r/A_a}=l/L$)
ψ_c dimensionless constriction resistance ($=R_{cs}k\sqrt{A_r}$)
ω relaxation parameter.

Subscripts
a asperity
c contact
cs constriction
i, j, k indexes for meshes in the x-, y-, z-directions, respectively
l large
t thin
1, 2 body (1) or (2).

Abbreviations
2-D two-dimensional
3-D three-dimensional
C coupled bodies
UC uncoupled bodies.

* Corresponding author.

0017–9310/99/$ - see front matter
PII: S0017–9310(98)00320–2

1. Introduction

Temperature is an important parameter for problems of friction [1, 2]. The investigation of temperatures by analytical solutions or numerical models depends on the adopted equations for characterizing the heat transfer at the body/body contact. Experimental studies [3–5] concerning dry friction, have shown that there exists a discontinuity of temperature at the interface of sliding bodies. This jump of temperature is a conclusive indication of the presence of a thermal contact resistance R_c. For stationary solids R_c has been widely investigated [6–12]. The relative mobility of bodies modifies the constriction of the heat flux lines and subsequently R_c value. Experimental studies [4, 5, 13] show that R_c decreases with the increase of velocity. This tendency has been confirmed by analytical solutions [14, 15] where a semi-infinite solid subjected to heat sources is considered. Another analytical solution, based on a semi-infinite body subjected to numerous rectangular or squared heat sources is also proposed [16].

The proposed analytical solutions consider a single smooth body subjected to a uniform heat flux. In practice, heat flux distribution at the real contact area is non uniform due to the presence of the asperity of the other solid.

In this paper, a three-dimensional numerical model that considers two bodies in sliding contact was developed. The modeled geometry consists of two bodies: one is smooth and moving at a velocity V, the other is fixed and comprises numerous asperities shaped as squares which are uniformly distributed over the contact plane. For the same values of the real and apparent contact area, a square-shaped asperity is equivalent to a circular one [11].

In this study, we are interested in the constriction phenomenon within solids, heat transfers through interstitial gaps are not taken into account. The steady-state temperatures and dimensionless thermal contact resistance ψ_c were calculated in terms of two parameters characterizing the surface (ε) and the displacement (V^*). Small values of ε down to 0.05 ($A_r/A_a = 25 \cdot 10^{-4}$) were examined. In order to validate the numerical calculations, we compare the model's results, considering only the smooth [solid (2)] subjected to a uniform heat flux (uncoupled case: *UC*) to those of the analytical solution [16] (see the Appendix).

It has been shown that the domain of calculation could be reduced as a function of V^*. The iterative procedure, used for the resolution of the discretized equations, is initialized by means of a one-directional analytical model. This allowed for a significant reduction of the computation time.

The choice of the appropriate mesh is important for this kind of problem. For this purpose, a study of the mesh is undertaken. Moreover, the influence of asperity elongation in terms of the thermal contact resistance is addressed.

2. Description of the problem and governing equations

The study is based on two sliding bodies (Fig. 1). Body (1) is rough, stationary and comprises numerous square-shaped asperities with height δ and width $2l$ uniformly distributed over the contact plane (space periodicity $= 2L$). Body (2) is smooth and moving at a velocity V. The heat transfer through the interstitial gap is assumed to be negligible. The boundaries of the bodies are in convective exchange with their surrounding media at temperature T_e. Heat transfer is three-dimensional and at steady-state $T(x, y, z)$. By considering the periodicity of asperities in the x-direction and the symmetry of heat transfer in the y-direction, the studied domain was limited to an elementary cell (Fig. 2). Using notations of this figure and noting that j refers to the subscript of the body ($j = 1$ or 2), equations governing heat transfer in a steady-state could be as follows:

Heat equation:

$$\frac{\partial^2 T_j}{\partial x^2} + \frac{\partial^2 T_j}{\partial y^2} + \frac{\partial^2 T_j}{\partial z_j^2} - \frac{V}{\alpha_j}\frac{\partial T_j}{\partial x} = 0 \quad (V = 0 \text{ for body 1}). \tag{1}$$

Periodicity and symmetry conditions:

$$T_j(-L, y, z_j) = T_j(L, y, z_j) \quad \text{(periodicity)} \tag{2}$$

$$\frac{\partial T_j}{\partial x}(-L, y, z_j) = \frac{\partial T_j}{\partial x}(L, y, z_j) \quad \text{(periodicity)} \tag{3}$$

$$\frac{\partial T_j}{\partial y}(x, 0 \text{ or } L, z_j) = 0 \quad \text{(symmetry)}. \tag{4}$$

Boundary conditions:

$$\frac{\partial T_1}{\partial x}(x, y, z_1) = 0 \quad (|x| = l, 0 \leqslant y \leqslant l, 0 \leqslant z_1 \leqslant \delta) \tag{5}$$

$$\frac{\partial T_1}{\partial y}(x, y, z_1) = 0 \quad (|x| \leqslant l, y = l, 0 \leqslant z_1 \leqslant \delta) \tag{6}$$

$$-k_j \frac{\partial T_j}{\partial z_j}(x, y, e_j) = h_j(T(x, y, e_j) - T_{e_j}) \tag{7}$$

$$\frac{\partial T_1}{\partial z_1}(x, y, \delta) = \frac{\partial T_2}{\partial z_2}(x, y, 0) = 0 \quad \begin{cases} l \leqslant |x| \leqslant L, & 0 \leqslant y \leqslant L \\ |x| \leqslant l, & l \leqslant y \leqslant L \end{cases}. \tag{8}$$

Contact equations (at A_r)

$$T_1(x, y, 0) = T_2(x, y, 0) \quad (|x| \leqslant l, 0 \leqslant y \leqslant l) \tag{9}$$

$$q_c = q_1(x, y) + q_2(x, y) \quad (|x| \leqslant l, 0 \leqslant y \leqslant l) \tag{10}$$

where

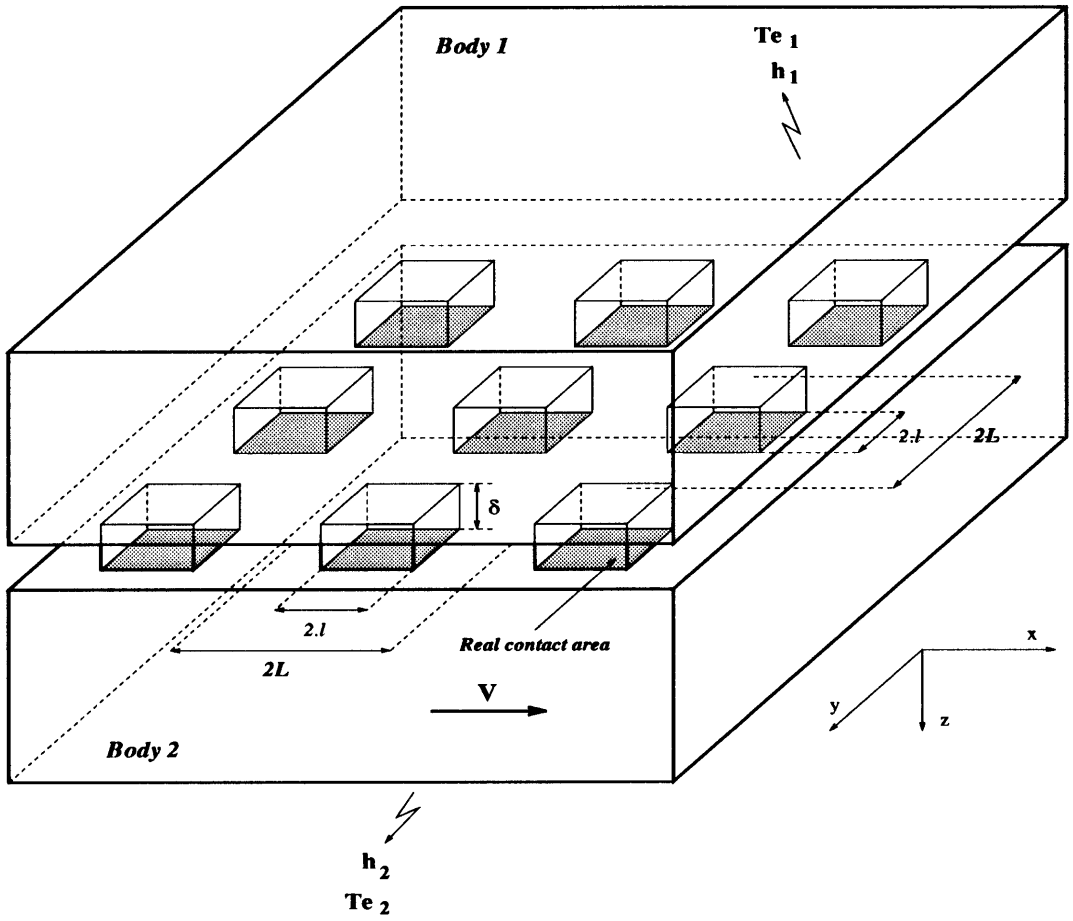

Fig. 1. Geometrical model.

$$q_j(x,y) = -k_j \frac{\partial T_j}{\partial z_j}(x,y,0). \tag{11}$$

In equation (10), the generated heat flux q_c is assumed to be uniform at the real contact area. This is not a limitation of the model.

3. Methodology of the numerical solution

For both bodies, heat transfer is three-dimensional up to the depths e'_j (limits of the constriction zone) and becomes one-dimensional beyond that (Fig. 3). Therefore, the domain of calculation is limited to the constriction zone and the remaining body is replaced with an equivalent thermal conductance h'_j:

$$h'_j = \frac{1}{\dfrac{1}{h_j} + \dfrac{e_j - e'_j}{k_j}} \tag{12}$$

e'_2 value is correlated to V^*:

$$e'_2 = \frac{5L}{\sqrt{V^*}} \quad (V^* > 6.3) \tag{13}$$

when $V^* \leqslant 6.3$ then e'_j is assumed to be equal to $2L$.

Heat transfer inside the reduced domain of bodies are calculated numerically, using the finite volume method [17]. Numerical equations are solved by the relaxation iterative method (SOR).

$$T^{(n+1)}_{i,j,k} = (1-\omega)T^{(n)}_{i,j,k} + \omega \tilde{T}_{i,j,k} \tag{14}$$

where superscripts (n) and $(n+1)$ represent successive iterates of the temperature solution and $\tilde{T}_{i,j,k}$ the partially corrected temperature between (n) and $(n+1)$ iterates, and ω the relaxation parameter.

The criterion for convergence can be specified as the absolute convergence criterion in the form:

$$|T^{(n+1)}_{i,j,k} - T^{(n)}_{i,j,k}| \leqslant \text{res} \tag{15}$$

where res is the residue.

The convective term $\partial T_2/\partial x$ in equation (1) is descre-

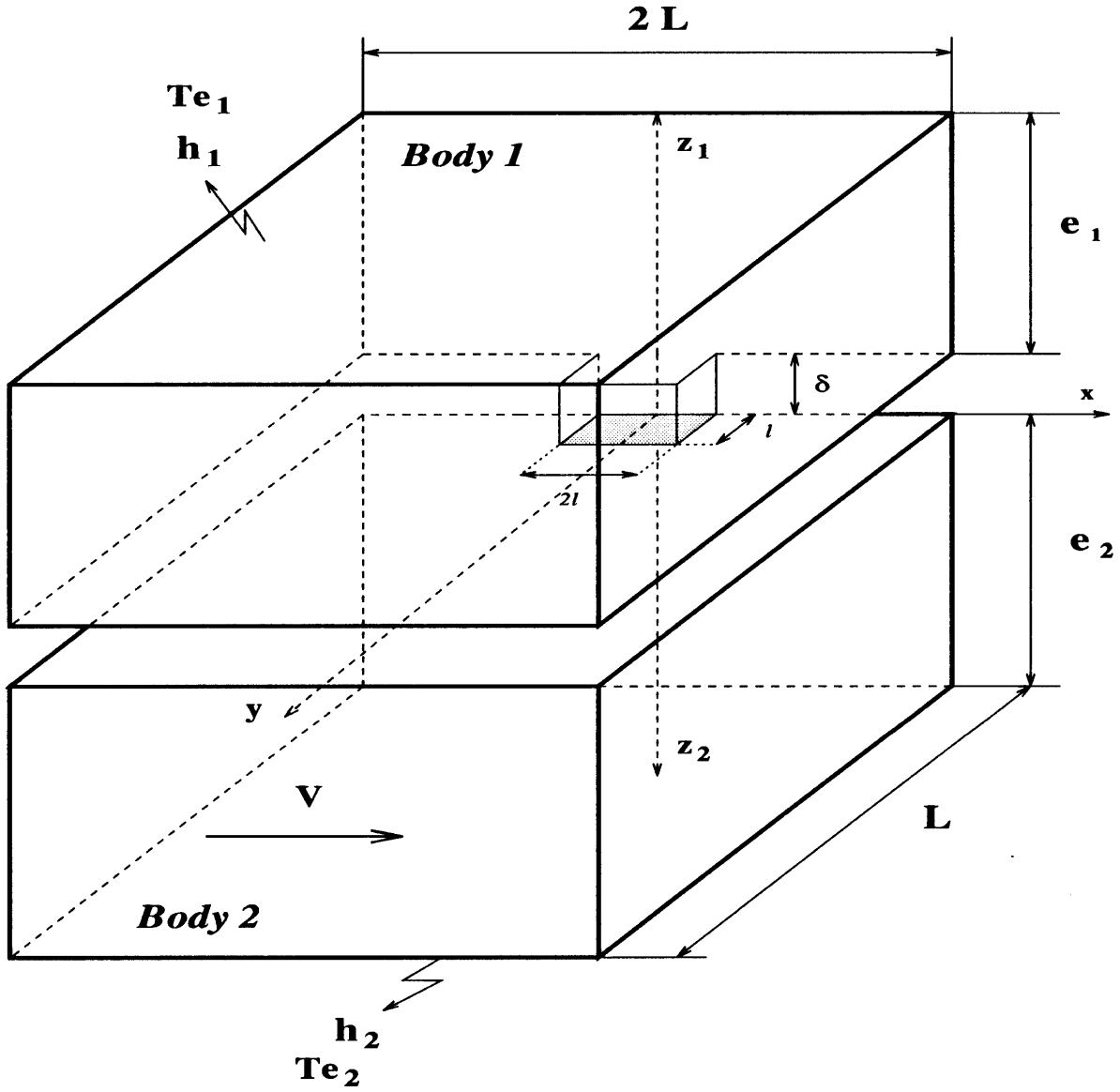

Fig. 2. Studied elementary cell.

tized by an upwind differencing scheme because V^* (equivalent to Peclet number) is high. In the case, ω must be less than 1. For the fixed body, $1 < \omega < 2$.

The value of the real area of contact is generally very small compared to that of the apparent area of contact. The mesh structure was adopted to be equal in both x- and y-directions, it comprises two zones (Fig. 4): a thin mesh at the vicinity of the contact and a larger one elsewhere. In the z-direction, a uniform mesh was adopted. A mesh study is given in Section 4.1.

Because the moving body homogenizes the thermal field in the direction of the displacement, the iterative procedure was initialized by using a one-dimensional model $T(z)$. Figure 5 provides the analogical scheme representing the above model whose solution is given as follows:

$$T_j(z) = T_{e_j} + Q_j R_j(z) \tag{16}$$

where

$$Q_1 = \frac{R_2}{R_1 + R_2} Q_c + \frac{T_{e2} - T_{e1}}{R_1 + R_2} \tag{17}$$

$$Q_2 = \frac{R_2}{R_1 + R_2} Q_c + \frac{T_{e1} - T_{e2}}{R_1 + R_2} \tag{18}$$

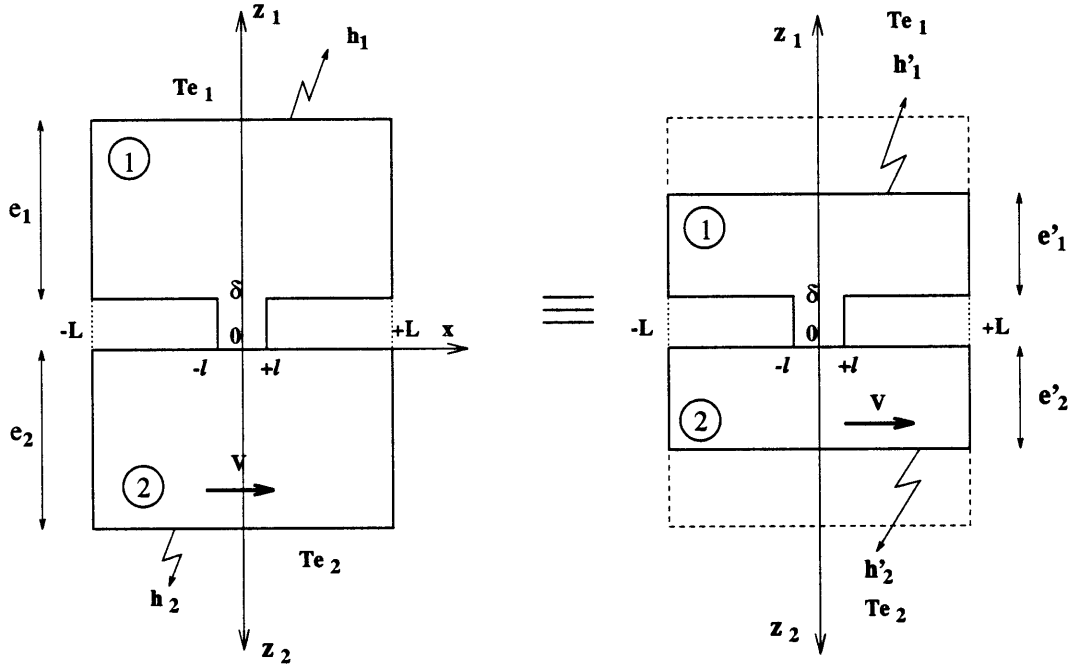

Fig. 3. Reduction of the modeled domain.

$$R_j(z) = \frac{z}{k_j A_a}, \quad R_j = \frac{e_j}{k_j A_a} + \frac{1}{h_j A_a}. \tag{19}$$

This allowed for a significant reduction in the computation time. In fact, the results have shown that iterates are reduced by 50% when compared to an initialization using a uniform temperature T_{e_j}.

4. Results and discussion

4.1. Influence of the mesh

The accurate determination of local temperatures, consequently of constriction resistances, for the examined moving contacts and particularly for small values of ε, necessitates a meticulous attention in the choice of the mesh. For these purposes, a study consisting of choosing the appropriate mesh is undertaken.

The grid numbers (N_{it}, N_{il} and N_k) are determined by comparing the values of the dimensionless constriction resistance ψ_c, provided by the numerical model for a smooth body subjected to a uniform flux at the real contact area, to those of any analytical model [16] (see the Appendix). Figure 6 provides the result of the comparison for $\varepsilon = 0.1$, and $V^* = 0$ and 20. For the same accuracy, this figure shows that the necessary number of grids for $V^* = 20$ is less than the one for $V^* = 0$. It is worth noting that from $N_k = 30$, variations of the relative error become negligible and that the couple ($N_{it} = 20$, $N_{il} = 10$) fits well. We have adopted these values for what follows. The number of meshes within the asperity is set to $N_a = 5$.

4.2. Temperatures

The local temperatures are very important for tribology (friction, wear) and mechanical studies (stress, strain,...). In order to validate the numerical calculations, we have studied the particular case where solid (2) is studied separately, subjected to uniform heat fluxes, and for which the analytical solution can be deduced from ref. [16] (see the Appendix).

The comparison of dimensionless surface temperatures (at the abscissa $y = 0$) for $\varepsilon = 0.1$ and $V^* = 0$, 60, 200 (Fig. 7), shows that the results are in agreement. The peak of dimensionless surface temperature decreases with increase in velocity and moves towards the exit of the contact.

The isothermal line inside body (2) ($|x| \leqslant L$, $y = 0{,}0 \leqslant z_2 \leqslant e'_2$), for $\varepsilon = 0.1$ and $V^* = 0$, 20, 60, and 100 were represented in Fig. 8. These figures make into evidence the thermal gradients that could play an important role in the thermomechanical aspects. It is worthwhile to mention that the flattening of temperatures becomes more important with the increase in velocity. For the above velocities, the temperature was completely flattened at the limit depth of the reduced domain e'_2. When V^* value increases, the peak of the dimensionless

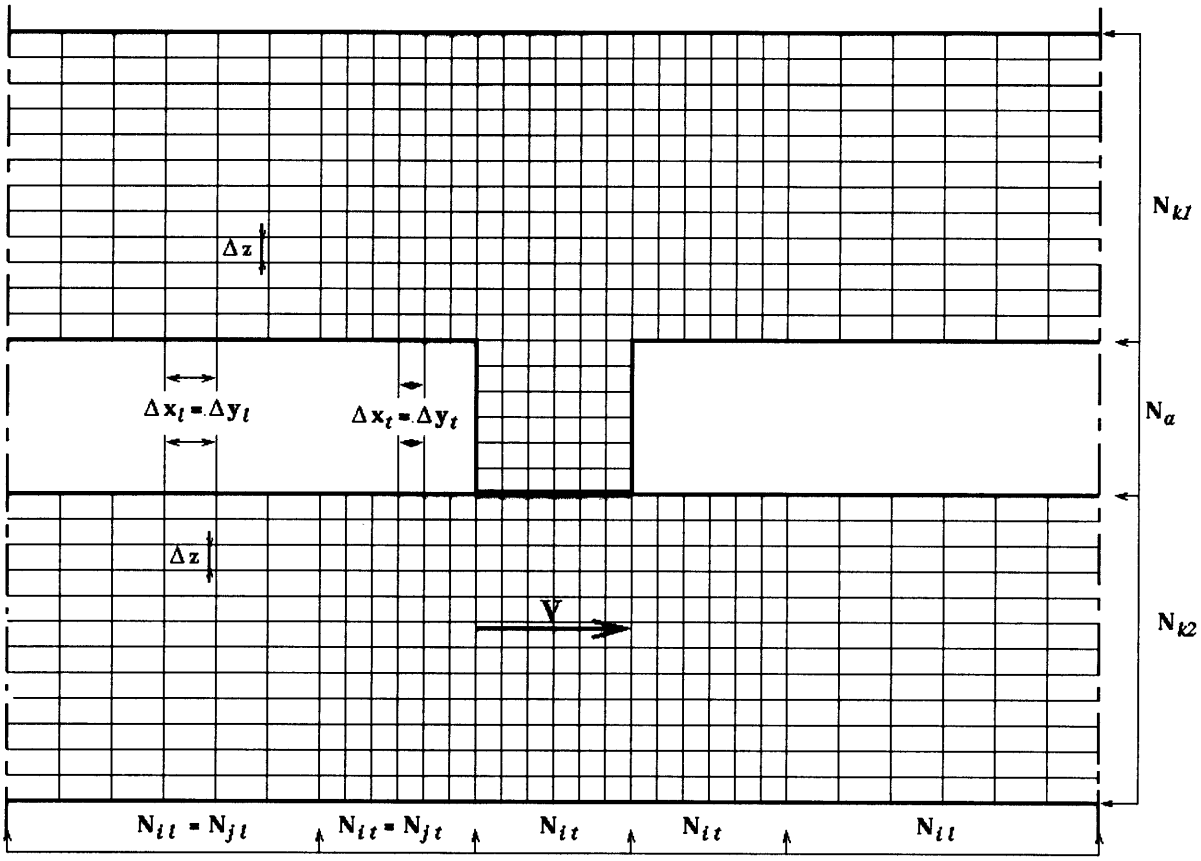

Fig. 4. Mesh structure.

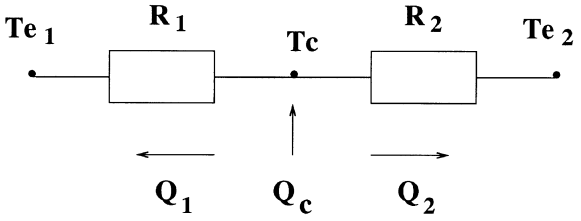

Fig. 5. Initialization procedure.

surface temperature decreases at the vicinity of the real contact area and the isothermal lines in the y-direction are flattened (Fig. 9).

4.3. Thermal contact resistance

Considering only solid media, the thermal contact resistance R_c of the studied geometry can be written as follows:

$$R_c = R_{cs1} + R_{a1} + R_{cs2} \tag{20}$$

where

$$R_{cs1} = \frac{\frac{1}{A_r}\iint_{A_r} T_1(x,y,\delta)\,dx\,dy - \frac{1}{A_a}\iint_{A_a} T_1(x,y,\delta)\,dx\,dy}{\iint_{A_r} q_1(x,y,\delta)\,dx\,dy} \tag{21}$$

$$R_{cs2} = \frac{\frac{1}{A_r}\iint_{A_r} T_2(x,y,0)\,dx\,dy - \frac{1}{A_a}\iint_{A_a} T_2(x,y,0)\,dx\,dy}{\iint_{A_r} q_2(x,y,0)\,dx\,dy} \tag{22}$$

$$R_{a1} = \frac{\frac{1}{A_r}\iint_{A_r} (T_1(x,y,0) - T_1(x,y,\delta))\,dx\,dy}{\iint_{A_r} q_1(x,y,0)\,dx\,dy}. \tag{23}$$

The thermal constriction resistance R_{cs} is the ratio of the difference between average temperatures of the real (A_r) and apparent (A_a) contact area, and the flux.

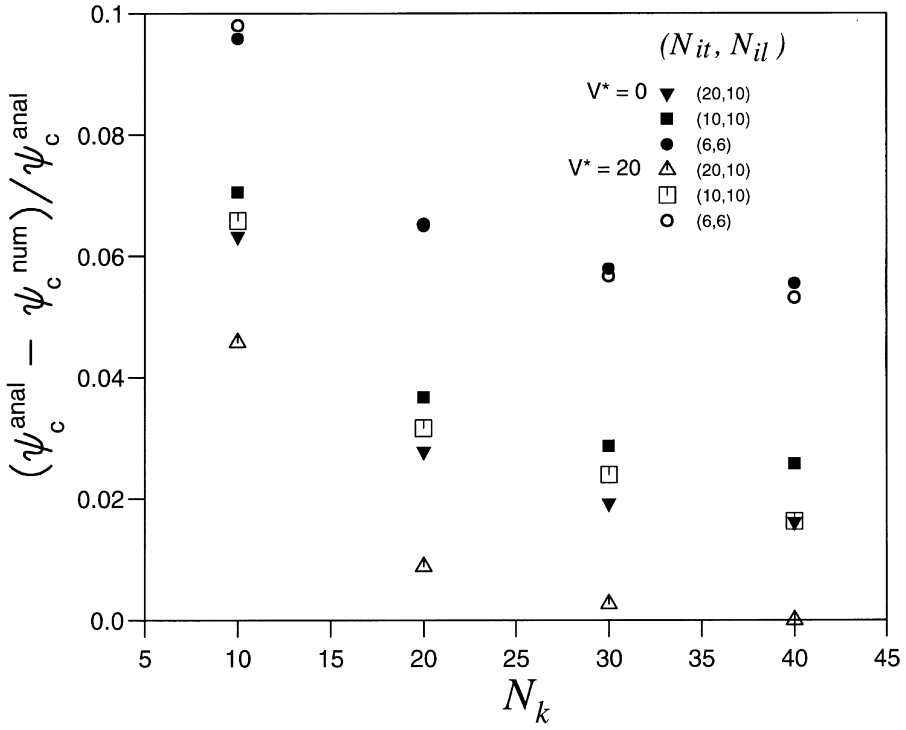

Fig. 6. Influence of the mesh.

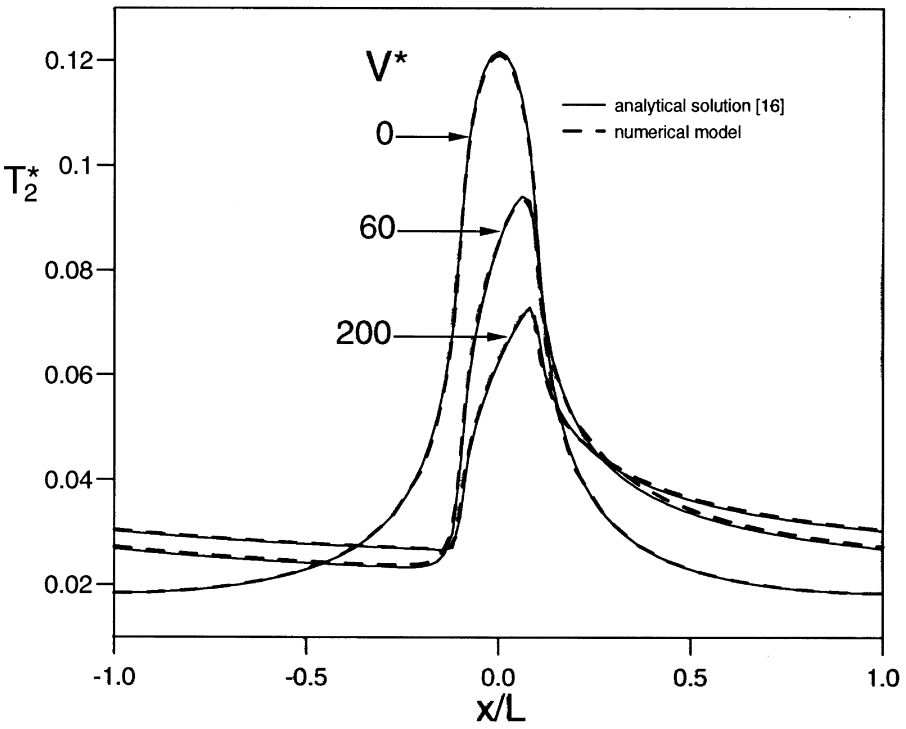

Fig. 7. Dimensionless surface temperature.

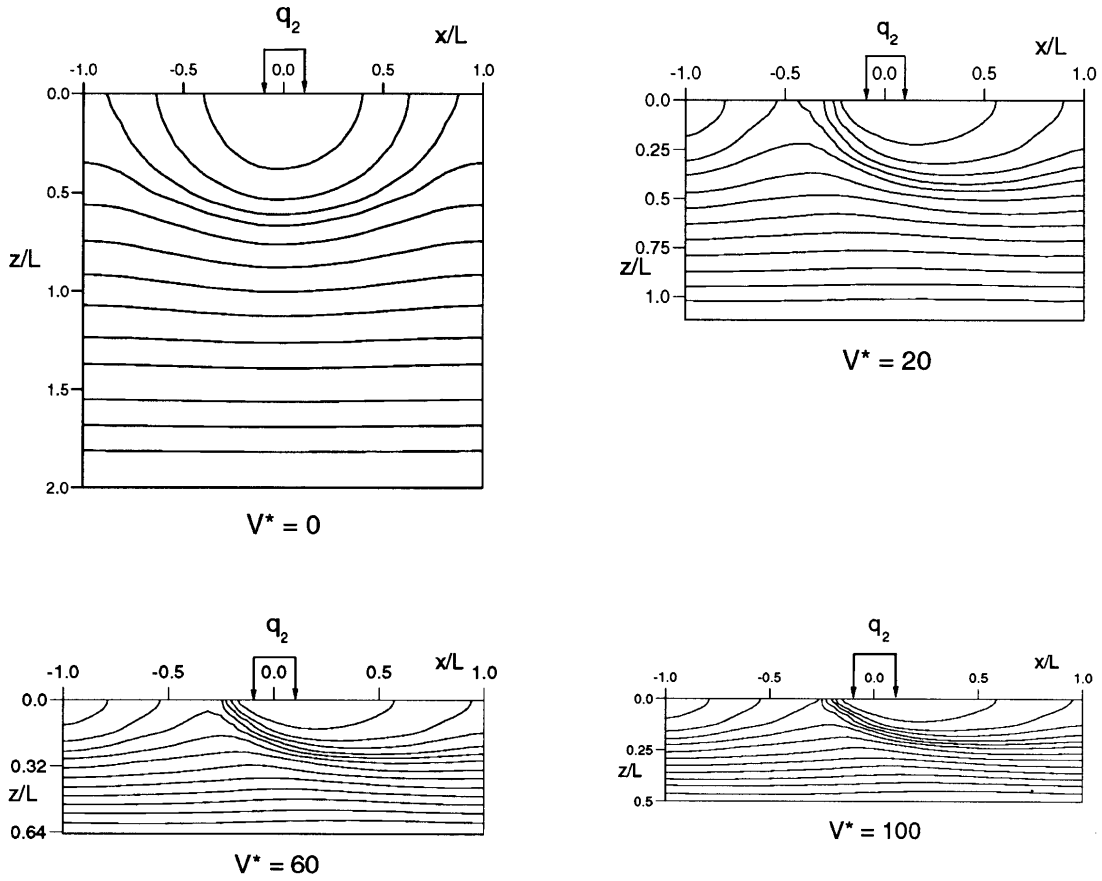

Fig. 8. Isothermal lines inside body (2) for $\varepsilon = 0.1$.

To illustrate the results, the dimensionless constriction resistance ψ_c is used:

$$\psi_c = R_{cs} k \sqrt{A_r}. \tag{24}$$

The expression of ψ_c in terms of ε and V^*, for a smooth single body subjected to square-shaped uniform heat fluxes sources, is given by [16] (see the Appendix).

Considering only solid (2), the results of ψ_{c2} as a function of ε and V^* are in agreement with those of the analytical solution (Fig. 10). Small values of ε down to 0.05, for the mesh adopted in Section 4.1, are examined. The ψ_{c2} value decreases with the increase in ε and V^*.

Table 1 illustrates the comparison of ψ_{c1} values, for body (1), in terms of ε ($V^* = 0$). In this case, equation (A1) is identical to that given by [9–11]. The numerical model provides ψ_c values slightly less than those of the analytical solution. This can be explained by the fact that the analytical solution uses a uniform flux distribution while in the numerical model the curve of temperature in terms of (x, y) at $z = \delta$ becomes flatter. It is known that the constriction is lower in the case of uniform temperature.

We considered the two bodies in actual contact (coupled case: *C*) in order to determine the dimensionless constriction resistance. The latter is then compared to the one where each solid is considered separately with a uniform heat flux at the real contact area (uncoupled case: *UC*). The results show that the obtained constriction for the smooth body is less than that for the uncoupled case (Table 2). The difference is about 4–5% at $V^* = 0$ and decreases with increase of velocity.

4.4. Influence of asperity elongation

The results of the dimensionless constriction resistance are compared to those of a two-dimensional numerical model [18] based on two bodies in relative motion. The first is smooth and moving at velocity V, the second is rough and fixed. The roughness is schematized by strip-shaped asperities perpendicular to the displacement. Table 3 shows the results of this comparison, for equal ratios of A_r/A_a and dimensionless velocity (V^*). As predicted, the two-dimensional dimensionless constriction

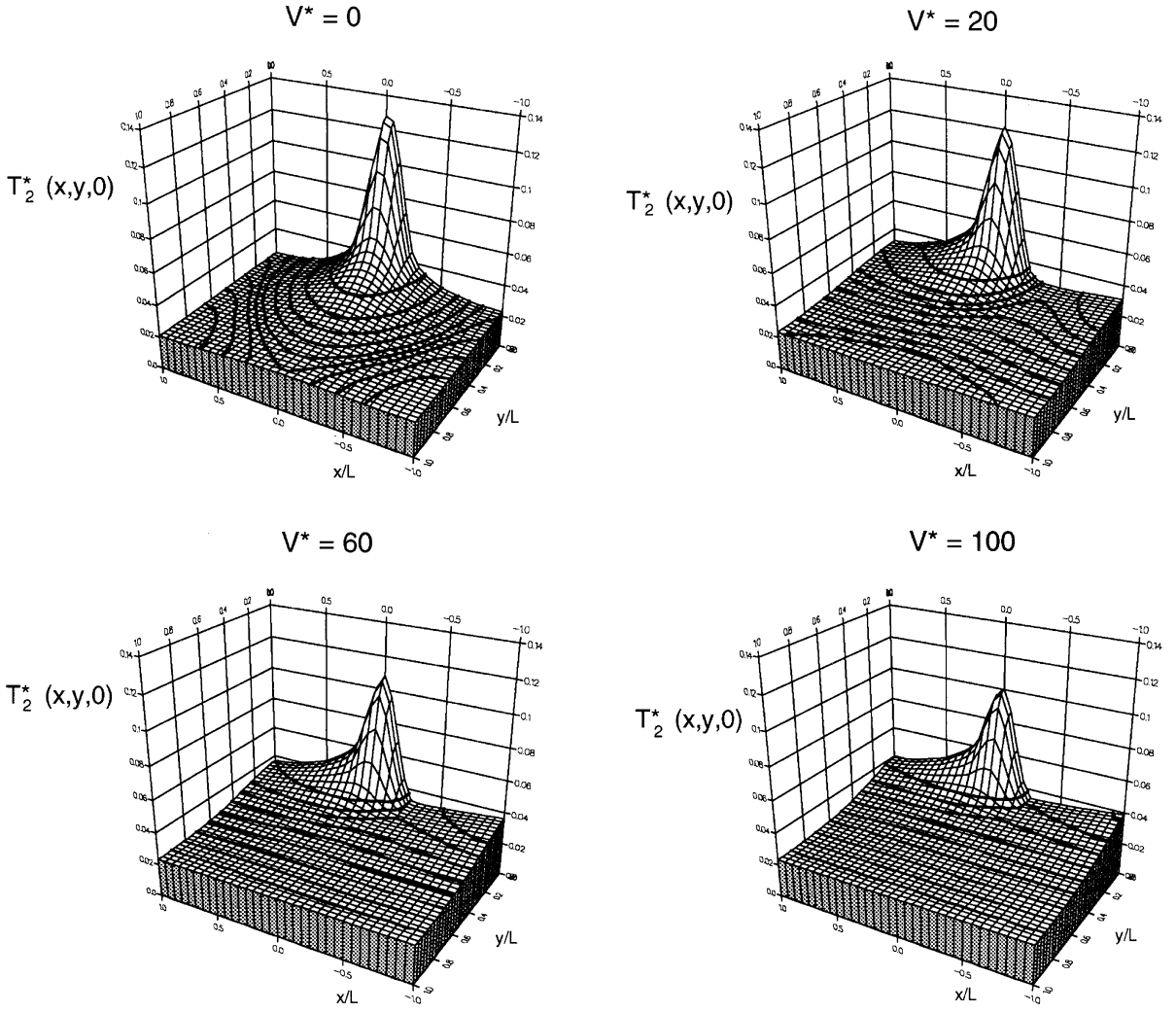

Fig. 9. Surface temperature at the contact plane of body (2).

resistance is two to four times less than the three-dimensional one for the studied values of ε and V^*.

5. Conclusions

A three-dimensional numerical model was developed to calculate the local temperatures and the thermal contact resistance between two bodies in relative motion.

In order to reduce the computation time, the domain of calculation was limited to the constriction zone and the iterative procedure was initialized by means of a one-directional analytical model.

It is worth mentioning that the numerical treatment of such a problem requires meticulous attention. Particularly, the mesh size Δz is proportional to $1/\sqrt{V^*}$.

It has been shown that: (i) the thermal contact resistance decreases while both parameters used (ε and V^*) increase, (ii) for coupled bodies, the thermal constriction is slightly less than that for uncoupled bodies.

For the same values of ε and V^*, the three-dimensional constriction resistance is two to four times more than the two-dimensional one.

Appendix

The analytical solution for a smooth semi-infinite body subjected to numerous square-shaped heat sources, moving at velocity V is proposed in [16].

The dimensionless constriction resistance is given as follows:

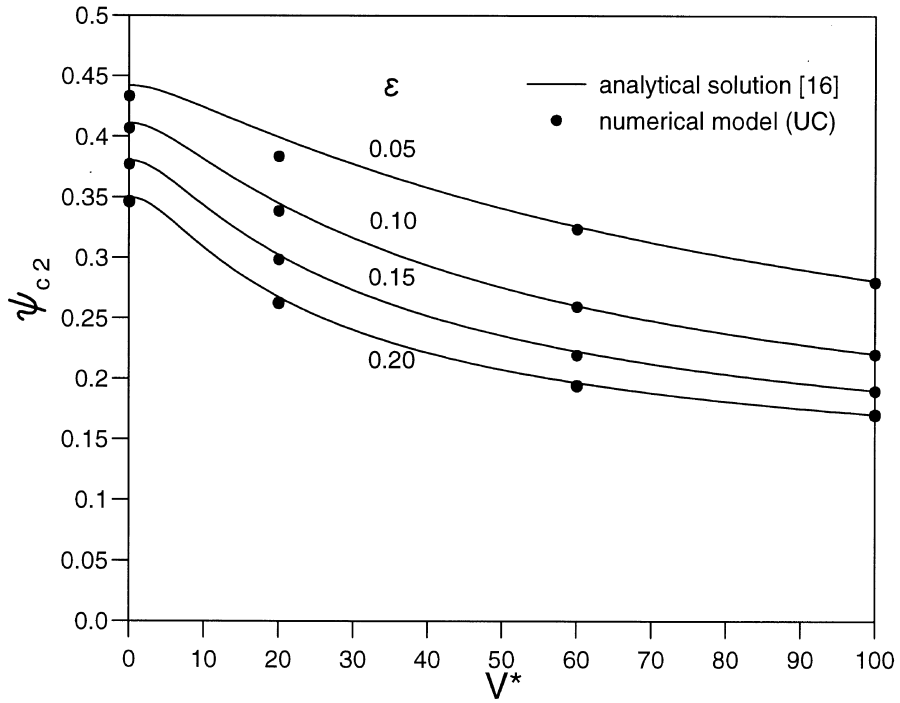

Fig. 10. Dimensionless constriction resistance evolution vs. ε and V^*.

Table 1
Comparison of ψ_{c1} values with those of the analytical solution [16]

ψ_{c1}							
$\varepsilon = 0.05$		$\varepsilon = 0.1$		$\varepsilon = 0.15$		$\varepsilon = 0.2$	
Equation (A1)	Num.	Equation (A1)	Num.	Equation (A1)	Num.	Equation (A1)	Num.
0.4421	0.4095	0.4112	0.3870	0.9805	0.3589	0.3500	0.3270

Table 2
Coupling effect on the dimensionless constriction resistance

ψ_{c2}								
	$\varepsilon = 0.05$		$\varepsilon = 0.1$		$\varepsilon = 0.15$		$\varepsilon = 0.2$	
V^*	C	UC	C	UC	C	UC	C	UC
0	0.4116	0.4333	0.3890	0.4069	0.3616	0.3771	0.3334	0.3469
20	0.3622	0.3836	0.3258	0.3386	0.2907	0.2985	0.2534	0.2624
60	0.3091	0.3237	0.2531	0.2595	0.2151	0.2192	0.1918	0.1940
100	0.2727	0.2797	0.2168	0.2198	0.1880	0.1896	0.1691	0.1700

Table 3
Influence of asperity elongation

	$\varepsilon = 0.1$		$\varepsilon = 0.15$		$\varepsilon = 0.2$	
V^*	$\psi_{2\text{-D}}$	$\psi_{3\text{-D}}$	$\psi_{2\text{-D}}$	$\psi_{3\text{-D}}$	$\psi_{2\text{-D}}$	$\psi_{3\text{-D}}$
0	0.1297	0.4069	0.1624	0.3771	0.1820	0.3469
20	0.0956	0.3386	0.1197	0.2985	0.1252	0.2624
60	0.0768	0.2595	0.0843	0.2192	0.0811	0.1940
100	0.0665	0.2198	0.0672	0.1896	0.0629	0.1700

$$\psi_c = \sum_{p=1}^{\infty} \frac{\sin^2(p\pi\varepsilon)}{\sqrt{2}\varepsilon(p\pi)^3} \sqrt{\frac{1}{\sqrt{1+(V^*/2p\pi)^2}} + \frac{1}{1+(V^*/2p\pi)^2}} + \sum_{n=1}^{\infty} \frac{\sin^2(n\pi\varepsilon)}{\varepsilon(n\pi)^3} + \sum_{p=1}^{\infty}\sum_{n=1}^{\infty} \frac{\sqrt{2}\sin^2(p\pi\varepsilon)\sin^2(n\pi\varepsilon)}{\xi^3(p\pi)^2(n\pi)^2\sqrt{(p\pi)^2+(n\pi)^2}} \times \sqrt{\frac{1}{\sqrt{1+[V^*p\pi/2[(p\pi)^2+(n\pi)^2]]^2}}} + \frac{1}{1+[V^*p\pi/2[(p\pi)^2+(n\pi)^2]]^2}. \quad \text{(A1)}$$

The dimensionless surface temperature for a semi-infinite body is given as follows:

$$T^*(\xi,\mu,0) = B_{00} + \sum_{n=1}^{\infty} \frac{2\varepsilon\sin(n\pi\varepsilon)\cos(n\pi\mu)}{(n\pi)^2} + \sum_{p=1}^{\infty} \frac{2\varepsilon\sin(p\pi\varepsilon)\cos(p\pi\xi-\gamma_{p0}/2)}{(p\pi)^2\sqrt{1+(V^*/2p\pi)^2}} + \sum_{p=1}^{\infty}\sum_{n=1}^{\infty} \frac{4\sin(p\pi\varepsilon)\sin(n\pi\varepsilon)\cos(n\pi\mu)\cos(p\pi\xi-\gamma_{pn}/2)}{(p\pi)(n\pi)\sqrt{(p\pi)^2+(n\pi)^2}\sqrt{1+[V^*p\pi/2[(p\pi)^2+(n\pi)^2]]^2}} \quad \text{(A2)}$$

where

$$\xi = x/L, \quad \mu = y/L, \quad T^* = (T-T_c)/(qL/k),$$

$$\gamma_{p0} = a\tan(V^*/2p\pi)$$

$$\gamma_{pn} = a\tan(V^*p\pi/2((p\pi)^2+(n\pi)^2)), \quad B_{00} = C\text{st.} \quad \text{(A3)}$$

In order to determine the temperatures within the studied finite medium, B_{00} is obtained by applying a Fourier boundary condition at the limit of the constriction zone ($z = e'_2$), beyond which the temperature is linear as a function of z:

$$B_{00} = \varepsilon^2(1/Bi'_2 + e'^*_2) \quad \text{(A4)}$$

where

$$e'^*_2 = e'_2/L, \quad Bi'_2 = h'_2L/k. \quad \text{(A5)}$$

References

[1] D. Play, M. Godet, Design on high performance dry bearing, Wear 41 (1977) 25–44.
[2] F.E. Kennedy, Thermal and thermomechanical effects in dry sliding, Wear 100 (1984) 453–476.
[3] F.F. Ling, T.E. Simkins, Measurement of pointwise juncture condition of temperature at the interface of two bodies in sliding contact, J. Basic Engineering (1963) 481–487.
[4] L. Mazo, B. Casagne, D. Badie-Levet, J.P. Bardon, Etude des conditions de liaison thermique dans le cas de frottement sec métal–plastique, Revue Générale de Thermique Fr. 204 (1978) 921–933.
[5] G.A. Berry, J.R. Barber, The division of frictional heat—a guide to the nature of sliding contact, ASME Journal of Tribology 106 (1984) 405–415.
[6] J.P. Bardon, Heat transfer at solid–solid interface: basic phenomenon, recent works, Proceedings of Eurotherm, vol. 4, Nancy, France, 1988, pp. 40–74.
[7] M. Cooper, B.B. Mikic, M.M. Yovanovich, Thermal contact conductance, Int. J. of Heat and Mass Transfer 12 (1969) 279–300.
[8] M. Laurent, Contribution à l'étude des résistances thermiques de contact, Thèse de Doctorat d'Etat, Lyon, 1969.
[9] A. Degiovanni, C. Moyne, Résistance thermique de contact en régime permanent. Influence de la géométrie du contact, Revue Générale de Thermique Fr. 334 (1989) 557–563.
[10] L.S. Fletcher, Recent developments in contact conductance heat transfer, ASME Journal of Heat Transfer 110 (1988) 1059–1070.
[11] K.J. Negus, M.M. Yovanovich, J.V. Beck, On the nondimensionalization of constriction resistance for semi-infinite heat flux tubes, ASME Journal of Heat Transfer, Technical notes 111 (1989) 804–807.
[12] M.M. Yovanovich, General expression for circular constriction resistances for arbitrary flux distribution, in: Proceedings of AIAA 13th Aerospace Sciences Meeting, Pasadena, CA, January 1976, pp. 381–396.
[13] J.J. Vullierme, J.J. Lagarde, H. Cordier, Etude de la résist-

ance de contact entre deux matériaux. Influence de la vitesse de glissement, Int. J. Heat Mass Transfer 22 (1979) 1209–1219.

[14] J.P. Bardon, Bases physiques des conditions de contact thermique imparfait entre milieux en glissement relatif, Revue Générale de Thermique Fr. 385 (1994) 86–91.

[15] N. Laraqi, Phénomène de constriction thermique dans les contacts glissants, Int. J. Heat Mass Transfer 39 (1996) 3717–3724.

[16] N. Laraqi, Velocity and relative contact size effects on the thermal constriction resistance in sliding solids, ASME J. Heat Transfer 119 (1997) 173–177.

[17] S.V. Patankar, Numerical Heat Transfer and Fluid Flow. Hemisphere, New York, 1980.

[18] B. Salti, N. Laraqi, Two-dimensional numerical model for calculation of the thermal contact resistance between two sliding solids, Int. J. Heat and Technology 15 (1997) 17–22.